

Role of sample geometry on nonlinear transport properties of the vortex solid in $\text{Bi}_2\text{Sr}_2\text{CaCu}_2\text{O}_8$

R. A. Doyle and S. F. W. R. Rycroft

Interdisciplinary Research Center in Superconductivity, University of Cambridge, Cambridge CB3 0HE, England

T. B. Doyle

Department of Physics, The University of Natal, Durban, King George V Avenue, Durban 4001, South Africa

E. Zeldov

Department of Condensed Matter Physics, The Weizmann Institute of Science, Rehovot 76100, Israel

T. Tamegai and S. Ooi

Department of Applied Physics, The University of Tokyo, Hongo, Bunkyo-ku, Tokyo, 113, Japan

(Received 16 January 1998)

Transport and magnetization measurements have been made on prism- and plate-shaped crystals of $\text{Bi}_2\text{Sr}_2\text{CaCu}_2\text{O}_8$. For fields below about 60 Oe the resistivity for the prism and plate specimens is approximately the same above the melting transition temperature. However below this temperature, for equivalent current densities, the (nonlinear) resistivity for the plate goes rapidly to zero, while for the prism it shows a pronounced tail. This behavior is discussed in relation to geometrical effects in the two specimens. It establishes that the nonlinear transport properties of plate-shaped crystals in this regime do not reflect bulk vortex pinning properties and strongly suggests that the vortex lattice melting is accompanied by vortex decoupling. [S0163-1829(98)04925-X]

It is now widely accepted that the vortex lattice in $\text{Bi}_2\text{Sr}_2\text{CaCu}_2\text{O}_8$ (BSCCO) undergoes a first-order melting transition at temperatures above about 40 K.^{1,2} In local² and in global³ magnetization measurements, this transition appears, respectively, as a sharp jump or as a rather broader step. For the platelike single-crystal specimens which are usually used in these measurements, the linear in- and out-of-plane resistivities disappear, within typical experimental sensitivity, at the “melting” transition.^{4–6} This suggests that, at melting, the vortex lattice becomes either an entangled vortex liquid with zero tilt modulus c_{44} or a “gas” of decoupled pancake vortices. The bulk vortex pinning behavior of the solid vortex phase is usually deduced from analysis of magnetization or nonlinear transport critical current measurements.^{4–8} These are, however, expected to be subject to surface pinning and to geometry-barrier and surface-barrier (SB) effects^{9–18} which may contribute significantly to the measured critical current density and nonlinear resistivity, especially at higher temperatures. The geometrical barrier^{9–14} (GB) for a plate specimen, in perpendicular applied field, has been theoretically established to be particularly strong for applied fields $H_a < 0.5H_{c1}$. The effect is predicted to produce, in the absence of bulk pinning, magnetic hysteresis and a corresponding critical current density,^{10,12,13} and accordingly also a critical transport current.¹⁹ Complicated edge or corner effects may extend the GB to fields well above H_{c1} .¹⁰ Direct experimental evidence for the GB effect has been found by Majer *et al.*¹¹ By polishing a plate-shaped single crystal to produce a triangular cross section or “prism,” they show that below the melting transition the relatively large magnetic hysteresis apparent in the platelet specimen is reduced to very small values in the prism. This suggests that the (magnetically determined) critical current

density in the plate specimen results almost entirely from the GB effect. This conclusion should also relate to critical imposed transport currents,¹⁹ although this prediction has not yet been experimentally verified. The GB effect has serious implications for the interpretation of magnetization and transport measurements in plate specimens in terms of bulk vortex pinning behavior, especially at higher temperatures where the bulk pinning is expected to be weak. Since there is a considerable interest in nonlinear transport behavior at low (and zero) applied fields for the interpretation of Kosterlitz-Thouless transitions,²⁰ current-induced vortex cutting,²¹ vortex-loop unbinding,²² and also bulk pinning parameters in platelike single-crystal specimens geometrical barrier effects must be taken into account. In this paper we report on the results of transport and isothermal magnetization measurements on both platelet- and prism-shaped single-crystal specimens of BSCCO. The results confirm that measurements on plate-shaped crystals are dominated by geometry effects at high temperatures and, in particular, that bulk vortex-lattice behavior cannot be obtained directly from the nonlinear transport properties of such specimens in this regime. The data also suggest strongly that the vortex phase above the melting transition is decoupled.

The starting material was selected from a batch of slightly overdoped single crystal $\text{Bi}_2\text{Sr}_2\text{CaCu}_2\text{O}_8$ ($T_c \approx 86$ K) which was grown using an infrared floating-zone furnace.²³ Single crystals with optically smooth parallel surfaces and thicknesses of several tens of microns were carefully cut into slabs. One of these was then gently polished (using 0.25 μm diamond grit), into a “prism” (as per Ref. 11) of dimensions 1052 $\mu\text{m} \times 190 \mu\text{m} \times 55 \mu\text{m}$. An adjacent slab with dimensions 1053 $\mu\text{m} \times 200 \mu\text{m} \times 13 \mu\text{m}$ was chosen to serve as the “platelet” sample. Schematic drawings of the

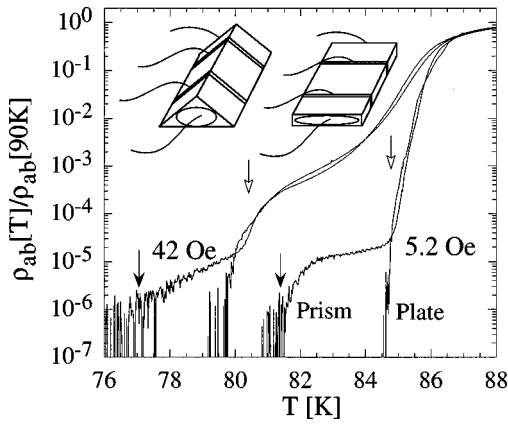


FIG. 1. Normalized resistivity $\rho_{ab}(T)/\rho_{ab}(90 \text{ K})$ of the prism- and plate-shaped samples at 1 mA for $H_a//c = 5.2$ and 42 Oe. Open arrows indicate both melting and the onset of the resistive tail for the prism. The closed arrows indicate where the tail vanishes below our sensitivity. The inset shows the sample geometry and contact configurations.

samples and their contact configurations are shown in the inset to Fig. 1. Silver epoxy contacts were fired onto the sample for 5 min at 420 °C in flowing oxygen. Contact resistances were measured to be between 1 and 2 Ω . The current contacts covered the entire ends of the crystal to ensure uniform in-plane current flow while the voltage contacts extended from the sample edge to its midline. The resistance was measured as a function of temperature at a frequency of 72 Hz (using low-noise, phase-sensitive detection) with the applied field parallel to the (thin) c axis of the crystals. Isothermal magnetization measurements were made using a QD-MPMS5 superconducting quantum interference device with due care to reduce the remnant field and a 3 cm scan length was used.

The experimental results for the reduced resistivity, $\rho(T)/\rho(90 \text{ K})$, at a transport current of 1 mA and in applied fields H_a (parallel to the c axis) of 5.2 and 42 Oe, are shown in Fig. 1 for both the plate and prism samples. The cross-sectional area of the plate is approximately two times smaller than that of the prism so that the current density is accordingly higher. The resistivity curves for the platelet and prism samples are almost coincident from above T_c down to a field-dependent temperature, marked by the open arrowheads, which is positively identified from the $M(H_a)$ curves (see below), as the melting temperature $T_m(H_a)$. At this temperature $\rho(T)$ for the plate drops rapidly to below our resolution. On the other hand, the resistance of the prism shows a marked change in slope and diverges rapidly from the behavior for the platelet. This is the central result of this paper. It suggests that although a large critical current appears in platelet-shaped samples immediately below melting, that this is due to a geometrical effect and unrelated to bulk pinning. The resistivity for the prism is significantly higher, and it disappears below our limit of resolution at a lower temperature marked by the closed arrows. At 5.2 Oe the difference is pronounced and the resistivity of the prism displays a “tail.” The evolution of this feature with applied field is shown for various fields in a range from 5.2 to 100 Oe in Fig. 2 where it is apparent that the effect disappears altogether for $H_a > 60$ Oe and $T < 75$ K.

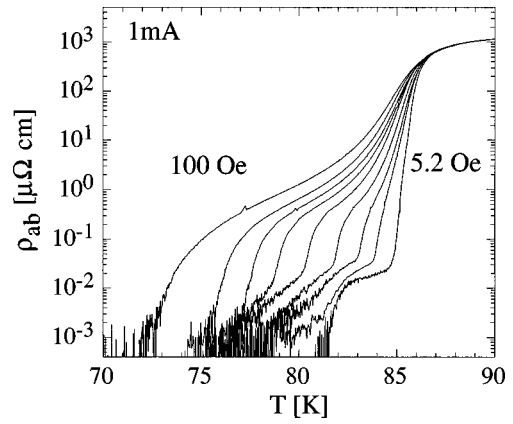


FIG. 2. Temperature dependence of the resistivity of the prism at applied fields of 5, 15, 23, 32, 42, 52, 62, 77, and 100 Oe for a current of 1 mA.

In Fig. 3 the transport current dependence of $\rho(T)$, at $H_a = 5.2$ and 42 Oe is shown for the prism. Significant non-linearity is apparent in the resistance at temperatures below the melting transition. There is also some qualitatively different nonlinearity in the $\rho(T)$ behavior for $H_a = 42$ Oe immediately above the melting transition. This has been noted elsewhere and has been ascribed to viscous effects (bulk pinning in the liquid phase).⁵ Recently however, it has been shown to be associated with surface rather than bulk currents.²⁴ However, apart from noting that the behavior above melting is very similar in the prism and platelet specimens, we focus on the behavior below melting in this report. Figure 3 shows that, in the limit of sufficiently small transport current, the $\rho(T)$ behavior for the prism apparently becomes more like that of the platelet (see Fig. 1). This suggests that the linear $\rho(T)$ vanishes immediately below the melting transition for any geometry³ and implies that a non-zero critical current, albeit much smaller than that observed in the plate, also appears immediately below melting in the prism. Alternatively, due to the finite sensitivity of the measurement, we may simply not be able to resolve the low linear resistivity which could be present at low currents at these high temperatures, either from weak bulk pinning or a SB.

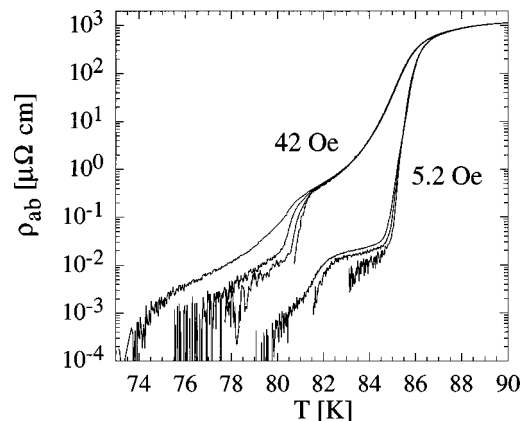


FIG. 3. Temperature dependence of the resistivity of the prism at 5.2 Oe for 300 μA , 1 and 3 mA and at 42 Oe for 100, 300 μA , 1 and 3 mA.

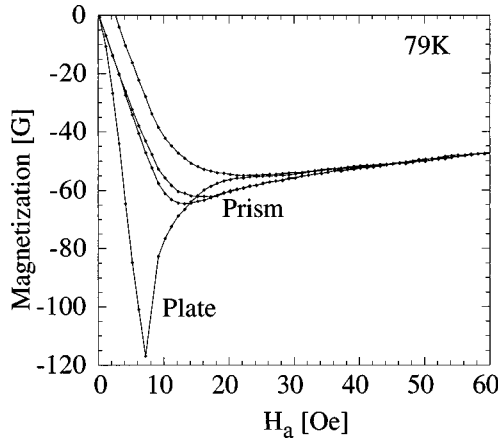


FIG. 4. Magnetization of the prism and plate at 79 K.

Magnetization measurements were carried out on the same samples to check that the differences in the transport behavior are not an artefact of polishing-related damage. The isothermal magnetization behavior $M(H_a)$ at $T=79$ K for the prism and platelet samples are presented in Fig. 4. These results are very similar to local magnetization measurements on a similar platelet and prism pair¹¹ and show that the hysteresis (and therefore critical current or nonlinear resistance) is significantly smaller in the prism than in the platelet, in agreement with the transport data. Although the prism shows some very small hysteresis in the vicinity of the penetration peak, the almost reversible behavior allows us to exclude polishing-induced damage (surface roughness and deformation) as contributing to these results. Such damage would be expected to enhance bulk and/or surface pinning and *increase* hysteresis, contrary to our observations.

Next we consider the physical origin of the differences between the two sample behaviors. The platelet specimen in Fig. 4 shows significant hysteresis and a magnetization loop similar to that predicted for the geometrical barrier^{10,12,13} for a specimen of this geometry with small or negligible bulk or surface pinning or SB effects. It is characterized by a delayed field for initial vortex penetration and hysteresis below applied fields of approximately $H_a=0.5H_{c1}$. At fields above about 25 Oe at 79 K, the behavior of the two samples is apparently very similar and, within experimental resolution, completely reversible and therefore approximately free from any effects of bulk pinning or surface barriers. Careful measurements have also been made to locate the melting transition. As an example, $M(H_a)$ loops for the prism at $T=77$ and 82 K are shown in Fig. 5. The melting fields, where the onset of broad steps in M are just discernible on the scale of the figure, are marked by open arrowheads. The solid arrows mark the applied field at which hysteresis, based on a criterion $\Delta M \leq 0.3$ G, apparently vanishes for each temperature. Inspection of Fig. 2, for $H_a \approx 62$ Oe and $H_a \approx 15$ Oe, shows satisfactory correspondence between these coordinates and those where the resistive tail for the prism specimen vanishes.

We now return to a detailed consideration of the implications of the divergence between the $\rho(T)$ curves for the platelet and the prism at the melting temperature. The above considerations show that the differences between the two geometries in both the transport and magnetization data are consistent with a dramatically reduced or vanishingly small

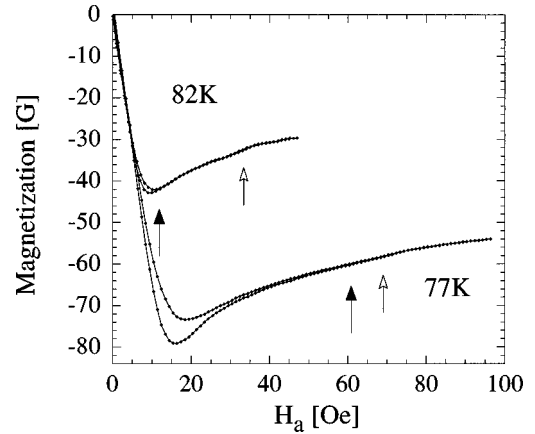


FIG. 5. Magnetization of the prism at 77 and 82 K. The open arrows mark the melting field while the solid arrows indicate the point where the hysteresis apparently disappears.

critical current in the prism relative to the plate. Moreover, the difference is clearly associated with specimen geometry and unlikely to result from bulk pinning, which should be comparable with or enhanced in the prism relative to the plate. In order to better understand these differences, we consider first the case of zero applied transport current. The spatial distributions of the equilibrium internal field and induction, which are related through the constitutive equilibrium relation $B[H_{rev}]$ for the superconductor, are different for the two geometries. In each geometry these field profiles are self-consistently dependent on magnetic boundary conditions and on the critical state which may include vortex-line tension forces which appear below the melting transition. These latter effects are significant over the entire volume of the prism and near the edges of the platelet. For the prism, the equilibrium (bulk-pinning-free) internal field and flux density profiles have a minimum along the specimen midline¹⁸ and a strong maximum along its edges. For the platelet geometry these fields have a “domelike” profile with a maximum along the specimen midline. In increasing applied fields in the range $H_a < 0.5H_{c1}$ the dome does not fill the specimen and is centered on the specimen midline.^{10,12,13} For H_a larger than a field of order $0.5H_{c1}$ the dome completely fills the specimen but still has a minimum along its edges. In decreasing applied field, for all fields down to zero, the dome continues to completely fill the specimen, thus allowing vortices to escape. The GB effect and the associated hysteresis in platelet (and disc) specimens is a direct consequence of these effects. Theoretical treatments¹²⁻¹⁴ for the GB in platelet and disc specimens make various simplifying assumptions to deal with the complex effects of vortex entry and expulsion from the sharp corners at the specimen edges. These treatments, in the absence of bulk pinning or SB effects, predict reversible $M(H_a)$ behavior for $H_a > 0.5H_{c1}$ (i.e., where the dome extends to the sample edges). The GB may, however, as a result of effects in, or due to, the sharp corners, persist in diminished magnitude to applied fields well above $0.5H_{c1}$.¹⁰ Now we consider the effect of transport currents. In the platelet geometry, applied transport currents in a transverse field distort the domelike flux profile and the critical currents can be calculated from critical conditions for entry and exit of vortices.¹⁹ For $H_a < 0.5H_{c1}$ platelet speci-

mens can carry remarkably large critical transport currents. Zeldov *et al.*¹⁰ estimate that critical currents associated with the GB are of order 10^6 A cm². Benkraouda and Clem¹⁹ obtain an expression for the transport critical current in strip geometry in this field regime which yields, for the present specimen dimensions, a critical current of up to 1 A. For fields above $H_a \approx 0.5H_{c1}$, a much reduced critical current is expected in the plate, consistent with the magnetization data (see Fig. 4).

We suggest, therefore, that the main differences between the transport properties in the platelet and prism geometries are due to the GB in the platelet sample. In this latter sample, the GB appears below T_m due to the onset of a nonzero line tension and nonzero c_{44} in the solid phase.²⁵ This results in a sharp drop in the resistivity.¹⁹ In the prism sample, in contrast, any GB leading to hysteresis is absent and as a result the measured resistivity below T_m is larger. Since the resistivity in the platelet sample below T_m is much lower than in the prism, we conclude that the nonlinear transport behavior in platelet specimens below freezing does not reflect bulk pinning properties. In addition to the GB, SB and bulk-pinning effects may also contribute to the above behavior. In particular, the SB effect is also expected to be dependent on vortex dimensionality and to increase below the melting temperature.¹⁷ Thus the possibility that the SB plays a role in the pronounced onset of the differences between the prism and platelet at melting is also qualitatively consistent with the present results. The SB, bulk pinning, or both may be

responsible for the nonlinear $I-V$ characteristics observed in the prism below T_m . Above T_m , geometrical barriers are significantly reduced in both geometries due to the decoupled nature of the liquid phase and thus the resistivities are comparable. Further, in this pancake gas phase, both bulk pinning and surface barriers are expected to be significantly reduced resulting in more linear characteristics.

In conclusion, the present work shows that the commonly assumed notion that the “irreversibility-line” defines the field-dependent temperature below which bulk pinning becomes significant should be applied with caution in platelet specimens at low fields of order approximately H_{c1} and for weak bulk pinning. In this regime both the nonlinear transport properties and hysteretic magnetization below the melting transition are predominantly determined by geometrical or surface barriers and do not reflect bulk properties, as is frequently assumed. The results are consistent with the suggestion that the vortices simultaneously decouple and melt, at least at temperatures above about 75 K.

We would like to thank D. T. Fuchs, A. M. Campbell, J. Keartland, and J. R. Clem for valuable discussions. T.B.D. wishes to thank the University of Natal and the Foundation Research and Development (RSA) for support. E.Z. acknowledges support by the Israel Science Foundation. This work is partly supported by the Grant-in-Aid for Scientific Research from the Ministry of Education, Science, Sports and Culture, Japan.

¹H. Pastoriza *et al.*, Phys. Rev. Lett. **72**, 2951 (1992).

²E. Zeldov *et al.*, Nature (London) **375**, 373 (1995).

³T. Hanaguri *et al.*, Physica C **256**, 111 (1996); S. Watauchi *et al.*, *ibid.* **259**, 383 (1996).

⁴D. T. Fuchs *et al.*, Phys. Rev. B **54**, R796 (1996).

⁵T. Tsuboi, T. Hanaguri, and A. Maeda, Phys. Rev. B **55**, R8709 (1997).

⁶D. T. Fuchs *et al.*, Phys. Rev. B **55**, R6156 (1997).

⁷G. Blatter *et al.*, Phys. Rev. B **54**, 72 (1996).

⁸S. L. Lee *et al.*, Phys. Rev. B **55**, 5666 (1997).

⁹M. V. Indenbom *et al.*, *Proceedings of the 7th International Workshop on Critical Currents in Superconductors*, Alpbach, Austria, 1994, edited by H. W. Weber (World Scientific, Singapore, 1994), p 327.

¹⁰E. Zeldov *et al.*, Phys. Rev. Lett. **73**, 1428 (1994).

¹¹D. Majer, E. Zeldov, and M. Konczykowski, Phys. Rev. Lett. **75**, 1166 (1995).

¹²T. B. Doyle and R. Labusch, J. Low Temp. Phys. **105**, 1207 (1996); T. B. Doyle, R. Labusch, and R. A. Doyle, Physica C **290**, 148 (1997).

¹³M. Benkraouda and J. R. Clem, Phys. Rev. B **53**, 5716 (1996).

¹⁴A. V. Kuznetsov, D. V. Eremenko, and V. N. Trofimov, Phys. Rev. B **56**, 9064 (1997).

¹⁵V. N. Kopylov *et al.*, Physica C **170**, 291 (1990).

¹⁶M. Konczykowski *et al.*, Phys. Rev. B **43**, 13 707 (1991).

¹⁷L. Burlachkov, Phys. Rev. B **47**, 8056 (1993); L. Burlachkov *et al.*, *ibid.* **50**, 16 770 (1994); L. Burlachkov *et al.*, *ibid.* **54**, 6750 (1996).

¹⁸N. Morozov *et al.*, Physica C **291**, 113 (1997).

¹⁹M. Benkraouda and J. R. Clem (unpublished).

²⁰S. Martin *et al.*, Phys. Rev. Lett. **62**, 677 (1989); S. N. Artemenko, I. G. Gorlova, and Yu. I. Latyshev, Phys. Lett. A **138**, 428 (1989).

²¹Y. M. Wan *et al.*, Phys. Rev. B **54**, 3602 (1996); T. Pe, M. Benkraouda, and J. R. Clem, *ibid.* **56**, 8289 (1997).

²²S. W. Pierson, Phys. Rev. B **55**, 14 536 (1997).

²³N. Motohira *et al.*, J. Ceram. Soc. Jpn. **97**, 994 (1989).

²⁴D. T. Fuchs *et al.*, Nature (London) **291**, 373 (1998).

²⁵M. V. Indenbom *et al.*, Physica C **235-240**, 201 (1994).